MOLEKUL
eISSN: 2503-0310

Articles
https://doi.org/10.20884/1.jm.2024.19.3.11037

The comparison of the Sensitivity Value of Gold Nanoparticles (AuNPs) between ANTAM and Commercial Gold Sources in the Detection of SARS-CoV-2: A Preliminary Study

Istianah[1], Agustina Vidiawati[2], Akhmad Irfan Alfiyan[3], Agustina Sus Andreani[4]*

[1]Chemistry Departement, IPB University, Dramaga, Bogor, West Java, Indonesia
[2]Chemistry Departement, State Islamic University Syarif Hidayatullah, Ciputat, South Tangerang, Indonesia
[3]Chemistry Departement, Jenderal Soedirman University, Purwokerto, Central Java, Indonesia
[4]Research Centre for Chemistry, National Research and Innovation Agency (BRIN), Serpong, South Tangerang, Indonesia

*Corresponding author email: agus147@brin.go.id

Received January 15, 2024; **Accepted** July 04, 2024; **Available online** November 20, 2024

ABSTRACT. Gold nanoparticles (AuNPs) have been developed as a colorimetric sensor to detect SARS-CoV-2 with surface modification using N-ethyl-N'-(3-(dimethylamino)propyl) carbodiimide/N-hydroxysuccinimide (EDC/NHS) and angiotensin-converting enzyme II (ACE-2). The gold sources used in the synthesis are produced by PT Aneka Tambang Indonesia (ANTAM) and commercial gold nanoparticles (AuNPs). This study compares the sensitivity values of ANTAM gold sources and commercial AuNPs in detecting SARS-CoV-2. The AuNPs-ANTAM detection test against the SARS-CoV-2 resulted in LoD and LoQ values of 5.38 ng/mL and 17.92 ng/mL, in the linearity curve range of 10 – 50 ng/mL, respectively. LoD and LoQ values of commercial AuNPs for detecting SARS-CoV-2, respectively, are 6.69 ng/mL and 22.31 ng/mL in the linearity curve range of 10 – 50 ng/mL. Based on the LoD and LoQ values, AuNPs-ANTAM is more sensitive than commercial AuNPs in detecting SARS-CoV-2 over the same range of linearity curves.

Keywords: ACE-2, colorimetry sensor, EDC/NHS, gold nanoparticles, SARS-CoV-2, surface Modifications

INTRODUCTION

After appearing in Wuhan, the capital of China's Hubei Province, in December 2019, the unprecedented coronavirus disease 2019 (COVID-19) has caused significant disruption to the world's health and economy (Sohrabi et al., 2020). Worldometers recorded the country with the highest death rate in the world caused by COVID-19 and Indonesia is in 20th position.

Various methods have been developed to detect COVID-19, such as Real-Time Polymerase Chain Reaction (RT-PCR) (Lan et al., 2020; Li et al., 2020), Computed Tomography (CT-imaging) (Fang et al., 2020), Enzyme-Linked Immunosorbent Assay (ELISA) (Adams et al., 2020) and Lateral Flow Immunoassay (LFIA) (Wen et al., 2020). However, some of these methods still have weaknesses, such as the RT-PCR method requires expensive instrumentation, skilled personnel, long completion times, complicated protocols, and the possibility of false negative results (Munne et al., 2021). The CT-imaging method requires analysis for a long time, high cost, and tends to have false positives and negatives (Liu et al., 2021). The ELISA method's results may be negative because the test is too early on the patient, so you must wait a few days to ensure the patient is infected with the virus. The LFIA is more expensive than ELISA and LFIA method test takes a long time on a large scale (Herawati, 2020).

Due to the shortcomings of the previously mentioned methods, a selective, fast, cost-effective, ready-to-use, and ultrasensitive method is needed, namely the colorimetric method. The colorimetric method is a direct visual detection method with color changes when influenced by external stimuli. This method is common and widespread because of its simplicity (Besharati et al., 2022).

Gold nanoparticles (AuNPs) are often used for colorimetric tests because they are easy to synthesize, low cost, simple, practical, and have unique optical properties (Karakuş et al., 2021). AuNPs have Surface Plasmon Resonance (SPR) characteristics; changes in SPR indicate a change in the shape and size of the nanoparticles. The interaction between AuNPs and the SARS-CoV-2 virus (the cause of COVID-19) is expected to change the size and shape of the AuNPs, consequently changing the color and SPR of the AuNPs. In the visible light absorption spectrum, specific SPR AuNPs appear at a wavelength of ~520 nm; this causes the AuNPs solution to turn red. However, absorption at these wavelengths can shift to red or blue, which depends on the shape, size, and

orientation of the nanoparticles, the distance between the nanoparticles, and the surrounding dielectric conditions (Ishikawa et al., 1996).

Since the Severe Acute Respiratory Syndrome (SARS) outbreak in 2002 – 2003, researchers have found that the SARS-CoV virus (the cause of SARS) can enter host cells by binding to Angiotensin Converting Enzyme-2 (ACE-2) as its receptor (Du et al., 2009). The spike protein is shaped like spikes sticking to the SARS-CoV virus's surface. Based on biochemical interaction studies and crystal structure analysis, it has a strong binding affinity with human ACE-2 (Li et al., 2005). Binds to the ACE-2 receptor, which helps the SARS-CoV virus enter its host cell. When compared, the spike protein of SARS-CoV-2 or the COVID-19 virus has 76.5% amino acid sequence similarities with SARS-CoV, and their spike proteins are truly homologous (Xu et al., 2020). This means that the two viruses have the same way of infecting their host cells.

This research was developing a colorimetric sensor in which AuNPs were modified with N-(3-Dimethylaminopropyl)-N' -ethylcarbodiimide hydrochloride/N-Hydroxysuccinimide (EDC/NHS) and ACE-2 to detect SARS-CoV-2. The AuNPs used came from different gold sources. The gold sources used in the synthesis are AuNPs from a gold bar with a purity of 99.99% and commercial AuNPs. This study compares the sensitivity values of AuNPs from both sources of gold in detecting SARS-CoV-2 to improve the effectiveness of virus detection and optimize the use of raw materials, based on the LoD and LoQ values in the same range of linearity curve.

EXPERIMENTAL SECTION

Materials

The materials used in this work include a gold bar with purity 99.99% was obtained from PT Aneka Tambang Indonesia (ANTAM), aquaregia solution (HCl 30% Mallinckrodt and concentrated HNO_3 Merck), AuNPs (Sigma-Aldrich 752568), tri-Sodium Citrate Dihydrate (Merck), ACE-2 (Sino Biological), EDC (≥98%, Sigma-Aldrich 03450), NHS (98%, Sigma-Aldrich 130672), Bovine Serum Albumin (BSA, ≥98%, Sigma-Aldrich 05470), Phosphate Buffer Solution (PBS 1.0 M) and SARS-CoV-2 (2019-nCoV) Spike S1-His Recombinant Protein (HPLC-verified, Cat:40591-V08H) from Sino Biological.

Synthesis of AuNPs-ANTAM

$HAuCl_4$ 1000 mg/L was prepared by dissolving 1000 mg ANTAM pure gold with 40 mL aquaregia solution (32 mL HCl 37% and 8 mL HNO_3 65%) then added distilled water until volume 1000 mL. $HAuCl_4$ concentration then varied from 0.05 – 0.20 M. The AuNPs-ANTAM in this work was synthesized by the solution of $HAuCl_4$ added to 0.005 – 0.05 M tri-sodium citrate in a volume ratio of 1:1 (5mL:5mL) and heated at 98 °C for 5 – 30 minutes. The color of the heated solution was observed visually as AuNPs and analyzed by UV-Vis spectrophotometry at a wavelength range of 300 – 800 nm. The optimum condition of AuNPs-ANTAM was used for further work.

Surface Modification of AuNPs with EDC/NHS and Determination of the Optimal Ratio of AuNPs-EDC/NHS

Prepare five microtubes, 1 mL of AuNPs was added into each microtube. Microtube 1 was used as a control (110 uL of distilled water), while microtubes 2, 3, 4, and 5 were each added with EDC/NHS at a ratio concentration of 4:1, 2:1, 1:1, and 0.5:1 (10 uL EDC and 100 μL NHS). Furthermore, the five microtubes were shaken at room temperature at 200 rpm for 30 minutes. The absorbance of the solution was measured using a UV-Vis spectrophotometer.

Surface Modification of AuNPs-EDC/NHS with ACE-2 and Determination of Optimal ACE-2 Concentration

AuNPs-EDC/NHS with optimal ratio were prepared in 5 microtubes (microtube one was added with 50 μL of distilled water as a control), while microtubes 2, 3, 4, and 5 were each added with 50 μL of ACE-2 with a variation of concentration of 0.005; 0.002; 0.001 and 0.0005 mg/µL. Next, shake at 200 rpm for 60 minutes at 37 °C. 10 μL of 1% BSA (m/v) in PBS was added to each microtube. After that, shake again for 15 minutes with a speed of 200 rpm at 37 °C. Then analyzed with a UV-Vis spectrophotometer with a wavelength range of 300 – 800 nm to determine the optimal concentration of ACE-2.

SARS-CoV-2 Detection

The SARS-CoV-2 spike antigen was diluted into 10, 20, 30, 40, and 50 ng/mL concentrations. AuNPs ACE-2 100 μL and SARS-CoV-2 with various concentrations were put into 96-well plates (AuNPs-ANTAM, commercial AuNPs, ACE-2 100 μL and distilled water 100 μL used as controls), then covered with aluminum foil and shaken for 10 minutes at 200 rpm at room temperature. The color of the solution changes to purple, indicating a successful reaction. Then, it is analyzed using an ELISA Reader at 300 – 800 nm. Absorbance value versus antigen concentration of SARS-CoV-2 spike is used to calculate calibration plots, LoD (limit of detection), and LoQ (limit quantity). The equation used is as follows:

$$SD = \frac{\sqrt{\Sigma(x1-\bar{x})}}{n-1}$$

$$LoD = \frac{3SD}{s}$$

$$LoQ = \frac{10SD}{s}$$

Notes:
SD = Standard deviation
s = Slope (from the standard curve linear regression equation)

Characterization

UV–Vis spectrophotometry (Agilent Cary 60) was used to analyze the absorbance of the AuNPs and other samples. For Fourier-transform infrared (FTIR; Thermo Scientific Nicolet iS-10) spectroscopy and field emission scanning electron microscopy (FESEM; Thermo Scientific Apreo 2) characterization, the

samples were dripped onto a silicon wafer of 1 × 1 cm and left overnight. After drying, FTIR measurement was conducted at a wavenumber of 500 – 4,000 cm^{-1}. For transmission electron microscopy (TEM; Tecnai G2 20S-Twin Function) characterization, copper grids were dipped in the samples and dried at room temperature.

RESULTS AND DISCUSSION

Synthesis of AuNPs-ANTAM

AuNPs-ANTAM synthesis was carried out under optimum conditions by varying the concentration of $HAuCl_4$, tri-sodium citrate, and reaction time. The higher the concentration of $HAuCl_4$, the more AuNPs formed; this can be seen from the higher SPR absorbance value. In **Figure 1a**. it can be seen that the $HAuCl_4$ 0.20 M has the greatest absorbance at 523 nm. **Figure 1b**. showed the absorbance of AuNPs with varying concentrations of tri-sodium citrate; the highest absorbance was produced at a concentration of 0.005 M, but the peak was widened. Therefore, the concentration of tri-sodium citrate used for synthesis is 0.010 M because the resulting SPR peak is narrower. Reaction times were varied from 5 to 30 minutes. Based on **Figure 1c**, the absorbance reaction times at 30 and 20 minutes are similar. The reaction time to be elected in the synthesis is 20 minutes because it is shorter, and the absorbance peak produced is similar from 30 minutes.

AuNPs-ANTAM was made by mixing tri-sodium citrate solution at optimum condition (5 mL of 0.010 M) with $HAuCl_4$ solution at optimum condition (5 mL of 0.20 M) into a test tube. The formation of AuNPs was indicated by a change in the color of the solution starting from colorless to red wine during the heating process at 98 °C for 20 minutes. The color change occurs due to the excitation of the surface plasmon nanoparticles. Identification of AuNP formation through UV-Vis spectrophotometer analysis indicated the presence of a maximum wavelength of around 500 – 600 nm depending on the particle size (Fazrin et al., 2020). AuNPs-ANTAM synthesized with sodium citrate at optimum conditions had a red wine color with an absorbance of 0.65 and had a surface plasmon resonance (SPR) wavelength at 523 nm (**Figure 2**).

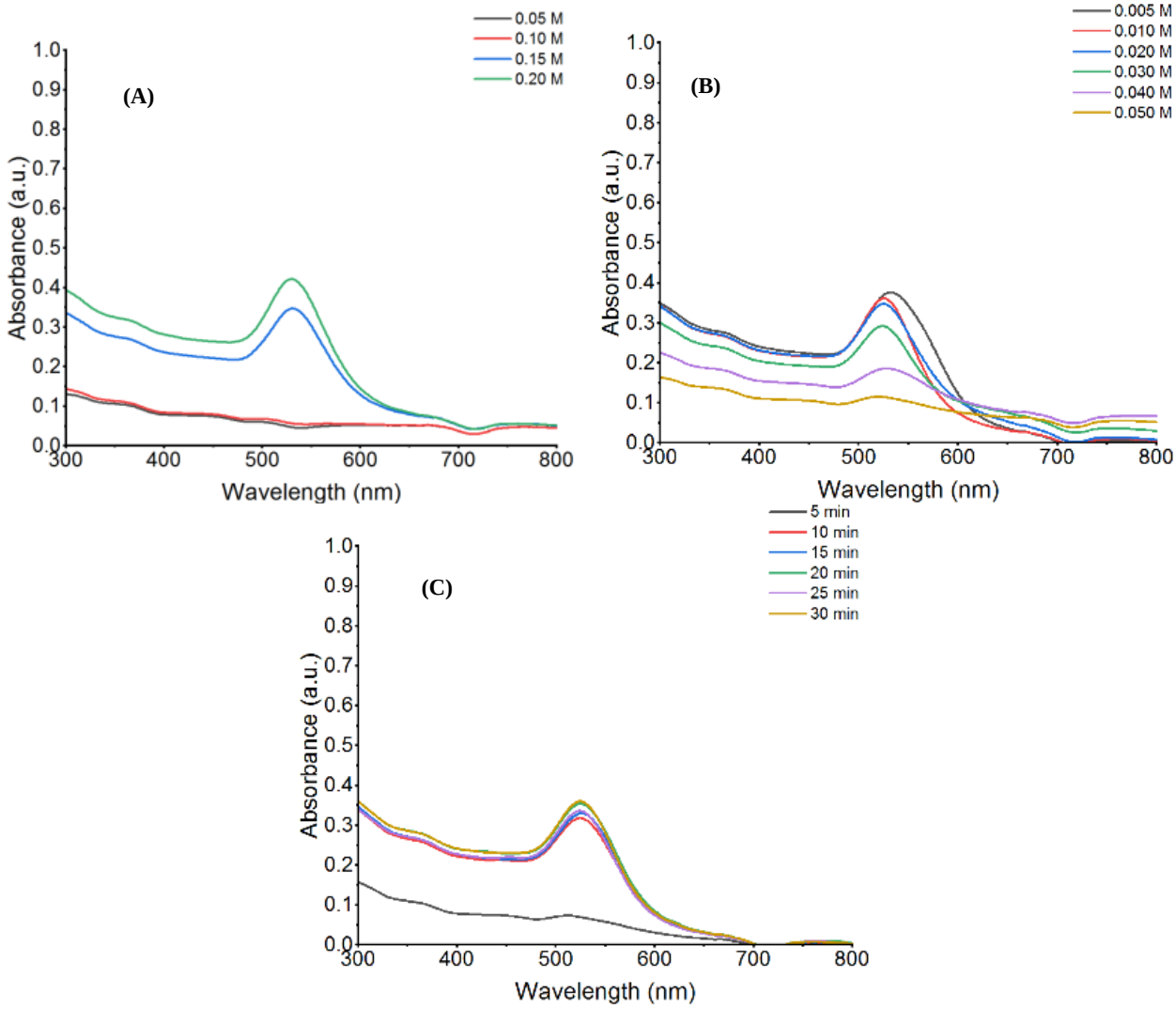

Figure 1. SPR Spectra of AuNPs at different (**A**) $HAuCl_4$ concentrations (**B**) citrate concentration and (**C**) reaction time.

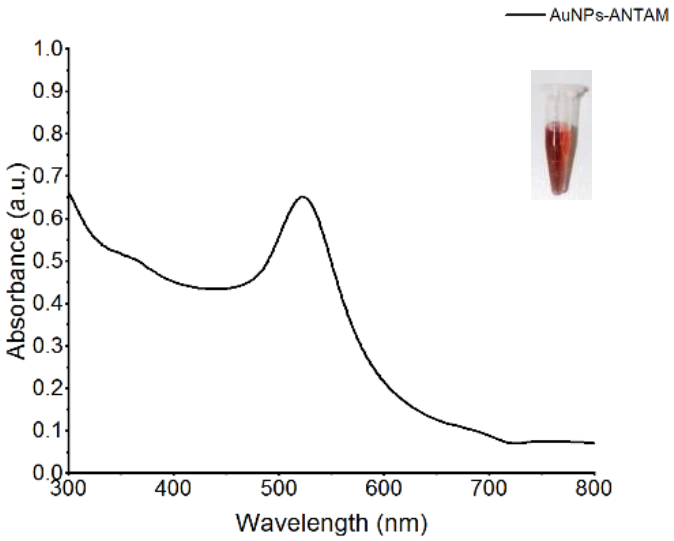

Figure 2. SPR Spectra of AuNPs-ANTAM at optimum condition.

Surface Modification of AuNPs with EDC/NHS and Determination of the Optimal Ratio of AuNPs-EDC/NHS

EDC/NHS was used to modify the surface of AuNPs. The function of EDC/NHS is to activate the carboxyl groups on the surface of AuNPs so that they can bind with the amine groups on the antibodies that will be attached to the surface of AuNPs (Raghav & Srivastava, 2016). After AuNPs were modified with EDC/NHS (AuNPs-EDC/NHS), AuNPs experienced a decrease in absorbance (**Figure 3**). The results showed that the decrease in absorbance was insignificant (about 17 – 28%), and there was no change in the color of the AuNPs. That means that after modification, AuNPs can maintain their physical properties. The best ratio for adding EDC/NHS is 2:1 because, at this ratio, the absorbance of AuNPs only decreases by 17%. The smaller decrease in the absorbance value indicates that the nanoparticles can maintain their physical and optical properties (Widyasari et al., 2022).

Surface Modification of AuNPs-EDC/NHS with ACE-2 and Determination of Optimal ACE-2 Concentration

AuNPs modified with ACE-2 aim to be selective in detecting SARS-CoV-2. But to combine AuNPs with ACE-2, it is necessary to do cross-linking because nanoparticles themselves are metals while ACE-2 is a biomolecule. The EDC/NHS is an intermediary between the nanoparticles and ACE-2, where the EDC initially binds to the carboxyl group, followed by forming amide bonds with the amino groups on the surface. NHS is used to stabilize the intermediary in this cross-linking reaction. After the nanoparticle binds to ACE-2, this EDC/NHS will be released (Vashist, 2012).

AuNPs-EDC/NHS was modified with 50 µL of ACE-2 with various concentrations. The results from the UV-Vis spectrophotometer analysis in **Figure 4** show that the most optimal concentration of ACE-2 is at a concentration of 0.0005 mg/µL because it has the smallest decrease in absorbance compared to the control only 18%, meaning that AuNPs modified with ACE-2 can still maintain their optical properties. The addition of ACE-2 causes a shift in the wavelength to 543 nm, and the color changes to purple.

SARS-CoV-2 Detection

The detection of SARS-CoV-2 was carried out at 534 nm for AuNPs-ANTAM and at 528 nm for commercial AuNPs. A linear response was noted in the concentration range of SARS-CoV-2 10 – 50 ng/mL (**Figure 5**). Limit of Detection (LoD) is the lowest amount of concentration of SARS-CoV-2 antigen that can be detected with a tool while Limit of Quantification (LoQ) is the amount of lowest concentration of SARS-CoV-2 antigen that can be measured accurately and precisely using equipment or instrument (Forootan et al. 2017; Santoso et al. 2021). The AuNPs-ANTAM detection test against the SARS-CoV-2 resulted in LoD and LoQ values of 5.38 ng/mL and 17.92 ng/mL, respectively. LoD and LoQ values of commercial AuNPs for detecting SARS-CoV-2 are 6.69 ng/mL and 22.31 ng/mL, respectively. Based on the LoD and LoQ values, AuNPs-ANTAM is more sensitive than commercial AuNPs in detecting SARS-CoV-2 over the same range of linearity curves.

Characterization

Characterization with FTIR was carried out on AuNPs-EDC/NHS samples and after the addition of ACE-2 (**Figure 6**) to understand the reaction mechanism that occurred. Changes in wave number can be seen in **Table 1**. After adding AuNPs by EDC/NHS, a C=O bond was formed between the NHS ester and the AuNPs surface (1780 cm^{-1}) and the N-O amine or succinimidyl ester group of NHS (1150 cm^{-1}). After reacting with ACE-2, the bond between the amine and ACE-2 produced a peak for the N-H amide group (1698 and 1550 cm^{-1}). The reaction mechanism can be seen in **Scheme 1**.

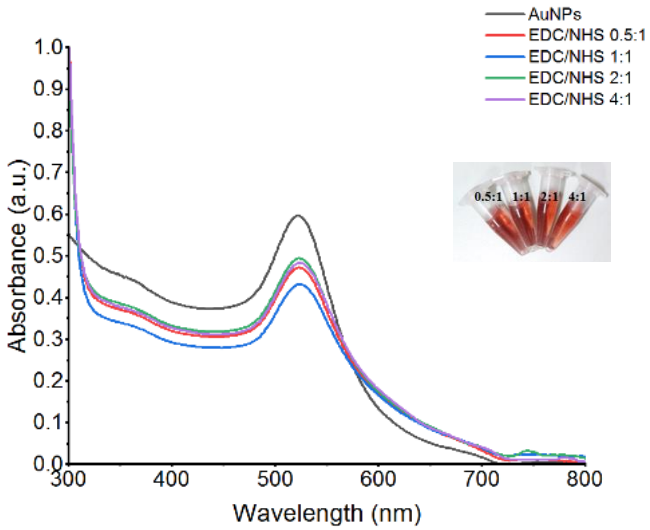

Figure 3. SPR spectra of AuNPs and AuNPs-EDC/NHS at different ratio.

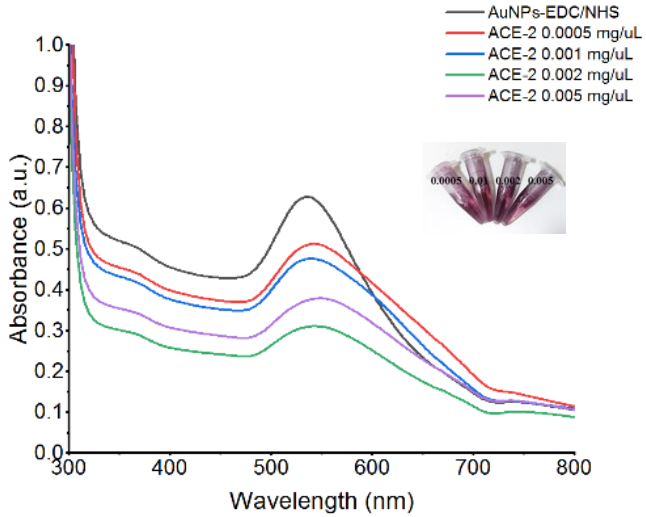

Figure 4. SPR spectra of AuNPs-EDC/NHS and ACE-2 at different concentration.

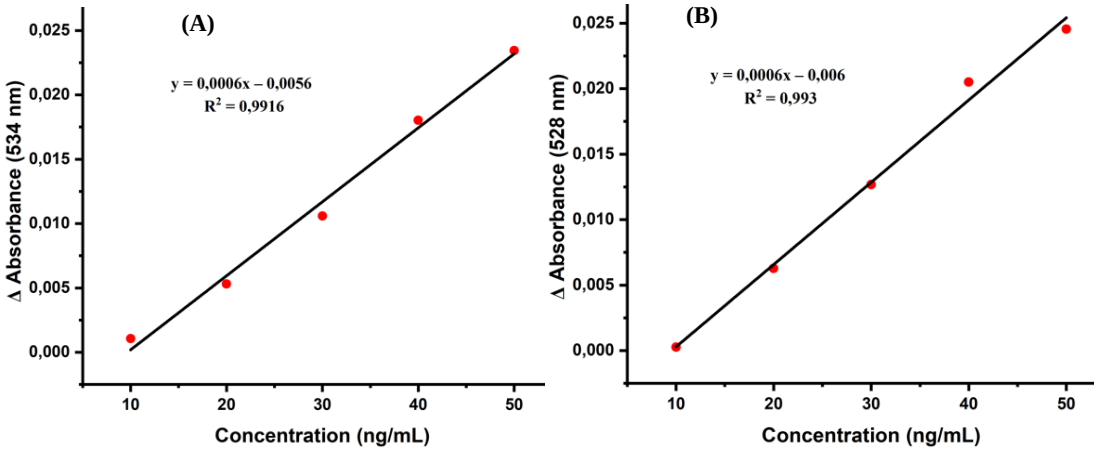

Figure 5. Calibration plot of Absorbance of (**A**) AuNPs-ANTAM (534 nm) (**B**) Commercial AuNPs (528 nm) versus the concentration SARS-CoV-2.

The SPR absorption between AuNPs, AuNPs-EDC/NHS, and AuNPs-ACE-2 was measured using a UV-Vis spectrophotometer. Based on **Figure 7**, AuNPs-ANTAM and commercial AuNPs experienced a decrease in absorbance peak when adding EDC/NHS. The addition of ACE-2 causes a decrease in absorbance and a shift in wavelength; this can be seen from the color of the solution changing to purple (**Figure 4**).

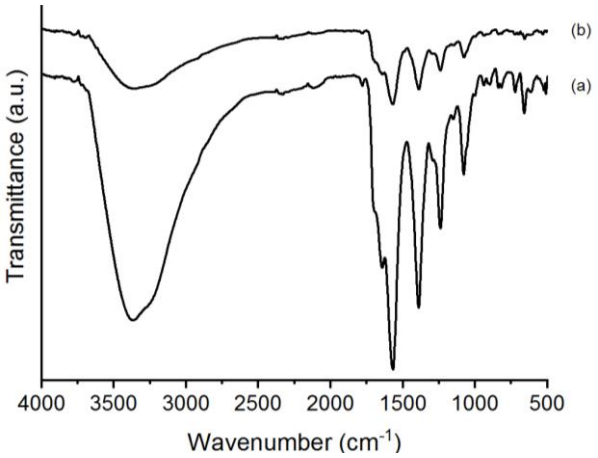

Figure 6. IR spectra of (a) AuNPs-EDC/NHS (b) AuNPs-EDC/NHS + ACE-2.

Table 1. Wavenumbers (cm^{-1}) of AuNPs-EDC/NHS, AuNPs-ACE-2

AuNPs-EDC/NHS	AuNPs-ACE-2	
3369	3349	O-H stretch of hydroxyl groups
1568	1568	Asymmetric carboxylate stretch
1390	1389	Symmetric stretching of the carboxylate groups of citrate molecules
1239	1293	Rotation of unbound hydroxyl groups
1780	1777	C=O NHS ester bound to the AuNPs surface
1150	1149	N-O amine / succinimidyl ester of NHS
	1698	N-H amide
	1550	

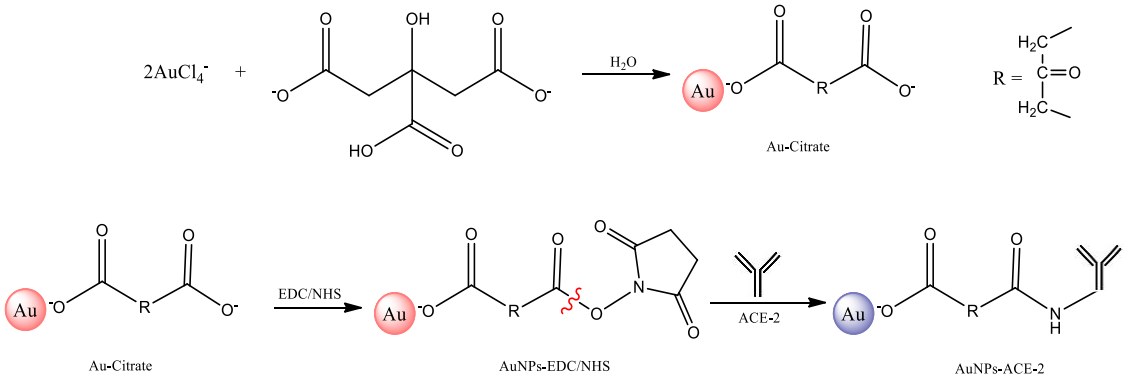

Scheme 1. Mechanism reaction of AuNPs-EDC/NHS + ACE-2.

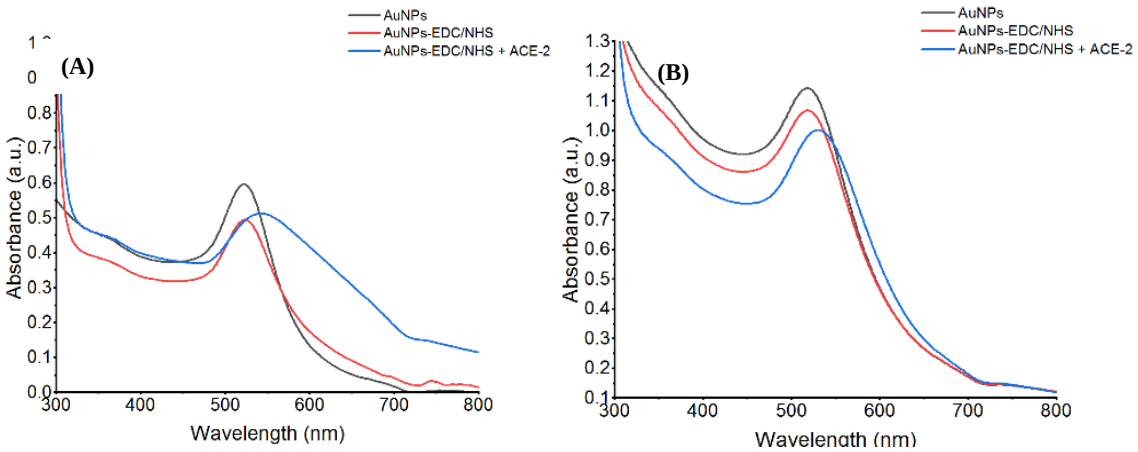

Figure 7.The difference in SPR absorbance between (**A**) AuNPs-ANTAM (**B**) commercial AuNPS after adding EDC/NHS and ACE-2 at optimum condition.

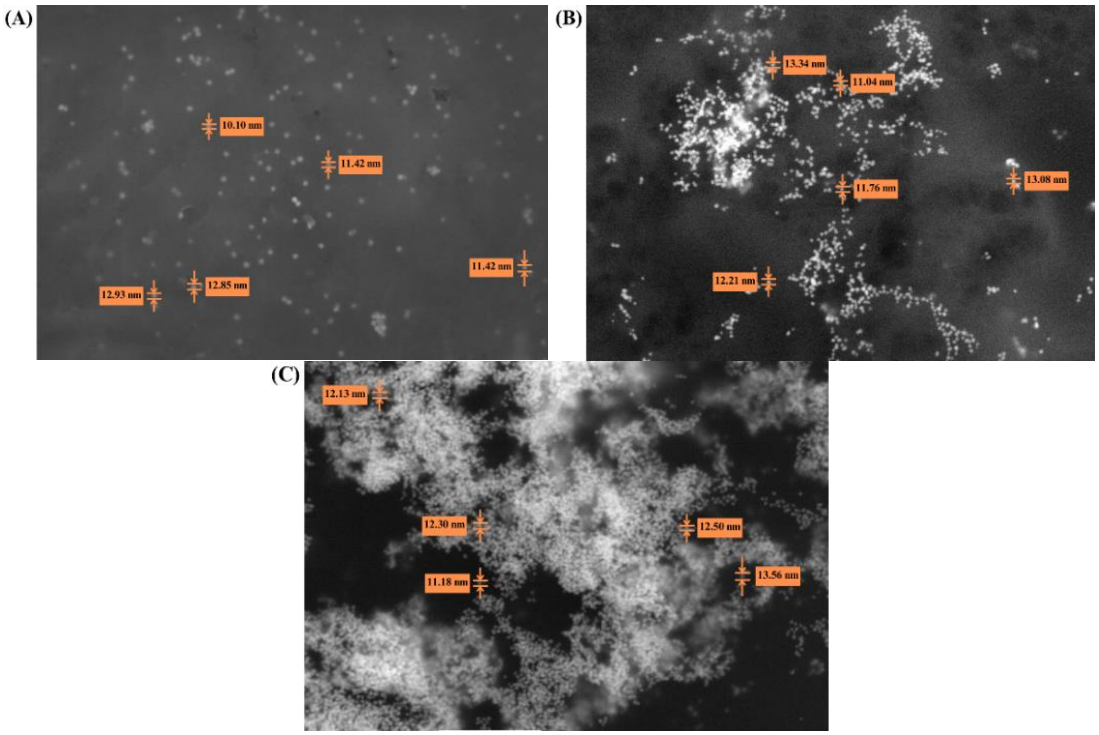

Figure 8. FESEM images of (**A**) AuNPs-ANTAM, (**B**) AuNPs-ACE-2, and (**C**) AuNPs-SARS-CoV-2.

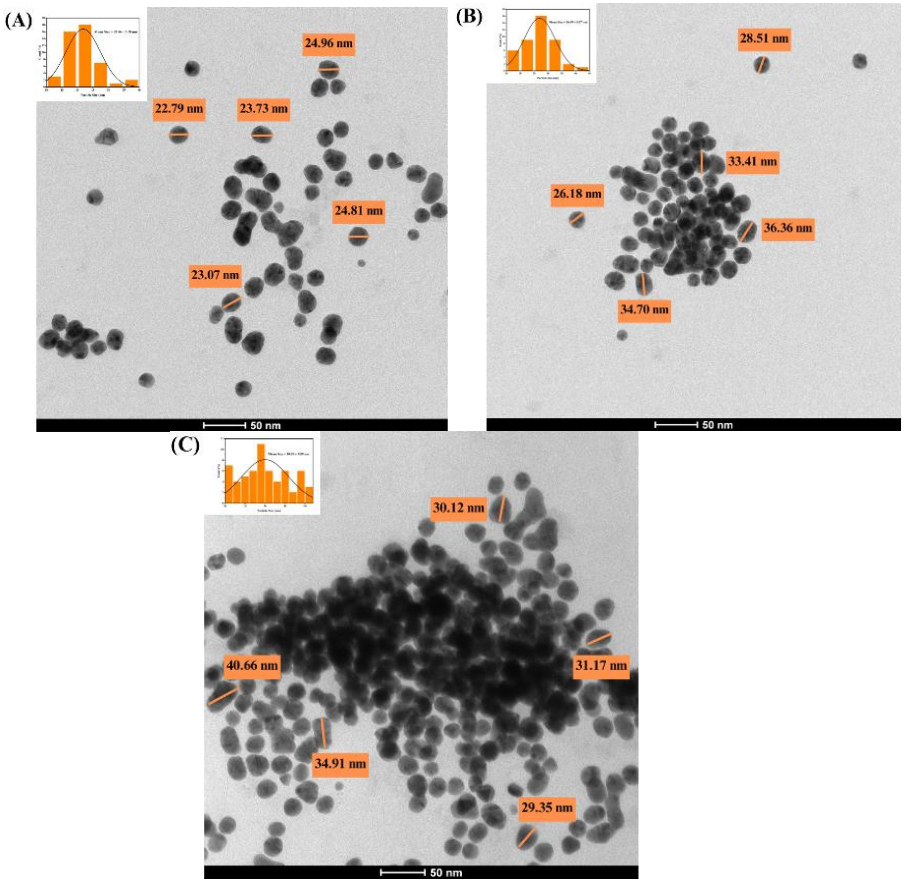

Figure 9. TEM images of (**A**) AuNPs-ANTAM, (**B**) AuNPs-ACE-2, and (**C**) AuNPs-SARS-CoV-2.

FESEM images show that ACE-2 and SARS-CoV-2 were uniformly distributed around AuNPs (**Figure 8**). There was no change in the morphology of the particles after reacting with ACE-2 and SARS-CoV-2 suggesting that the structural integrity of AuNPs is maintained even after the incorporation of ACE-2 and SARS-CoV-2. The FESEM images support the conclusion that the synthesized AuNPs are well-

dispersed without significant aggregation (Fatimah et al., 2021; Hidayat et al., 2022). The particle size was characterized using TEM and calculated using the ImageJ application. TEM images reveal the morphology of AuNPs were spherical with a uniform size distribution and there was no change in morphology when particles reacted with ACE-2 and SARS-CoV-2 (**Figure 9**). There was an increase in particle size after adding ACE-2 and SARS-CoV-2. The particle sizes of the AuNPs-ANTAM, AuNPs-ACE-2, and AuNPs-SARS-CoV-2 were 21.86 ± 5.58 nm, 26.99 ± 5.57 nm, and 30.03 ± 5.89 nm, respectively.

CONCLUSIONS

Surface modification of AuNPs with EDC/NHS and ACE-2 to detect SARS-CoV-2 has been successfully carried out. Modification with EDC/NHS at a ratio of 2:1 and decrease in absorbance of 17%. In surface modification with ACE-2, the optimum concentration of ACE-2 was 0.0005 mg/uL, with a decreased absorbance of 18% and a shift in SPR to 543 nm. The sensitivity of AuNPs-ANTAM and commercial AuNPs to detect SARS-CoV-2 was determined by LoD and LoQ values. The AuNPs-ANTAM is more sensitive in detecting SARS-CoV-2 over the same range of linearity curves (10 – 50 ng/mL) than commercial AuNPs, with LoD and LoQ values, respectively, 5.38 ng/mL and 17.92 ng/mL. Meanwhile, the LoD and LoQ values of commercial AuNPs, respectively, are 6.69 ng/mL and 22.31 ng/mL. Characterization by FTIR proved to be EDC/NHS and ACE-2 was covalently bound to the AuNPs surface. The particle sizes of the AuNPs-ANTAM, AuNPs-ACE-2, and AuNPs-SARS-CoV-2 were 21.86 ± 5.58 nm, 26.99 ± 5.57 nm, and 30.03 ± 5.89 nm, respectively.

AUTHORSHIP CONTRIBUTION STATEMENTS

Istianah: data curation, investigation, formal analysis, writing-original draft, and writing-review. Agustina Vidiawati: data curation, investigation, formal analysis, and writing-review. Akhmad Irfan Alfiyan: data curation, investigation, formal analysis, and writing-review. Agustina Sus Andreani: conceptualization, formal analysis, funding acquisition, investigation, methodology, supervision, validation, writing-review and editing. ASA is the main contributor in this manuscript.

ACKNOWLEDGMENTS

This research would like to acknowledge funding from the RP-OR Kesehatan (6/III.9/HK/2024), National Research and Innovation Agency (BRIN). The authors would also like to acknowledge the facilities: scientific and technical support from Advanced Characterization Laboratories Serpong, National Research and Innovation Agency (BRIN) through E-Layanan Sains, Badan Riset dan Inovasi Nasional.

REFERENCES

Adams, E. R., Ainsworth, M., Anand, R., Andersson, M. I., Auckland, K., Baillie, J. K., Whitehouse, J. (2020). Antibody testing for COVID-19: A Report from the National COVID Scientific Advisory Panel. *Wellcome Open Research*, *5*, 139. https://doi.org/10.12688/wellcomeopenres.15927.1

Besharati, M., Tabrizi, M. A., Molaabasi, F., Saber, R., Shamsipur, M., Hamedi, J., & Hosseinkhani, S. (2022). Novel enzyme-based electrochemical and colorimetric biosensors for tetracycline monitoring in milk. *Biotechnology and Applied Biochemistry*, *69*(1), 41–50. https://doi.org/10.1002/bab.2078

Du, L., He, Y., Zhou, Y., Liu, S., Zheng, B. J., & Jiang, S. (2009). The spike protein of SARS-CoV - A target for vaccine and therapeutic development. *Nature Reviews Microbiology*, *7*(3), 226–236. https://doi.org/10.1038/nrmicro2090

Fang, Y., Zhang, H., Xie, J., Lin, M., Ying, L., Pang, P., & Ji, W. (2020). Sensitivity of Chest CT for COVID-19: Comparison to RT-PCR. *Radiology*, *296*(2), E115–E117. https://doi.org/10.1148/radiol.2020200432

Fatimah, I., Citradewi, P. W., Yahya, A., Nugroho, B. H., Hidayat, H., Purwiandono, G., Sagadevan, S., Mohd Ghazali, S. A., & Ibrahim, S. (2021). Biosynthesized gold nanoparticles-doped hydroxyapatite as antibacterial and antioxidant nanocomposite. *Materials Research Express, 8*(11), 115003. https://doi.org/10.1088/2053-1591/ac3309

Fazrin, E. I., Naviardianti, A. I., Wyantuti, S., Gaffar, S., & Hartati, Y. W. (2020). Review: Sintesis dan karakterisasi nanopartikel emas (AuNP) serta konjugasi AuNP dengan DNA dalam aplikasi biosensor elektrokimia (Review: Synthesis and characterization of gold nanoparticles (AuNP) and conjugation of AuNP with DNA in electrochemical biosensor applications). *PENDIPA Journal of Science Education*, *4*(2), 21–39. https://doi.org/10.33369/pendipa.4.2.21-39

Forootan, A., Sjöback, R., Björkman, J., Sjögreen, B., Linz, L., & Kubista, M. (2017). Methods to determine the limit of detection and limit of quantification in quantitative real-time PCR (qPCR). *Biomolecular Detection and Quantification*, *12*(April), 1–6. https://doi.org/10.1016/j.bdq.2017.04.001

Herawati, N. (2020). Jenis-jenis metode rapid-test untuk deteksi virus SARS-CoV-2. *BioTrends*, *11*(1), 11–20.

Hidayat, H., Purwiandono, G., Tohari, T., Nugroho, B., Jauhari, M., Widyaputra, S. & Fatimah, I. (2022). Antibacterial and photocatalytic activity of visible-light-induced synthesized gold nanoparticles by using Lantana camara flower

extract. *Green Processing and Synthesis*, *11*(1), 1072-1082. https://doi.org/10.1515/gps-2022-0091

Ishikawa, H., Ida, T., & Kimura, K. (1996). Plasmon absorption of gold nanoparticles and their morphologies observed by AFM. *Surface Review and Letters*, *03*(01), 1153–1156. https://doi.org/10.1142/S0218625X96002060

Karakuş, E., Erdemir, E., Demirbilek, N., & Liv, L. (2021). Colorimetric and electrochemical detection of SARS-CoV-2 spike antigen with a gold nanoparticle-based biosensor. *Analytica Chimica Acta*, *1182*. https://doi.org/10.1016/j.aca.2021.338939

Lan, L., Xu, D., Ye, G., Xia, C., Wang, S., Li, Y., & Xu, H. (2020). Positive RT-PCR Test results in patients recovered from COVID-19. *JAMA - Journal of the American Medical Association*, *323*(15), 1502–1503. https://doi.org/10.1001/jama.2020.2783

Li, F., Li, W., Farzan, M., & Harrison, S. C. (2005). Structural biology: Structure of SARS coronavirus spike receptor-binding domain complexed with receptor. *Science*, *309*(5742), 1864–1868. https://doi.org/10.1126/science.1116480

Li, Y., Hu, Y., Yu, Y., Zhang, X., Li, B., Wu, J., Li, J., Wu, Y., Xia, X., Tang, H., & Xu, J. (2020). Positive result of Sars-Cov-2 in faeces and sputum from discharged patients with COVID-19 in Yiwu, China. *Journal of Medical Virology*, *92*(10), 1938–1947. https://doi.org/10.1002/jmv.25905

Liu, J., Yang, X., Zhu, Y., Zhu, Y., Liu, J., Zeng, X., & Li, H. (2021). Diagnostic value of chest computed tomography imaging for COVID-19 based on reverse transcription-polymerase chain reaction: a meta-analysis. *Infectious Diseases of Poverty*, *10*(1), 1–10. https://doi.org/10.1186/s40249-021-00910-8

Munne, K., Bhanothu, V., Bhor, V., Patel, V., Mahale, S. D., & Pande, S. (2021). Detection of SARS-CoV-2 infection by RT-PCR test: factors influencing interpretation of results. *VirusDisease*, *32*(2), 187–189. https://doi.org/10.1007/s13337-021-00692-5

Santoso, K., Herowati, U. K., Rotinsulu, D. A., Murtini, S., Ridwan, M. Y., Hikman, D. W., Zahid, A., Wicaksono, A., Nugraha, A. B., Afiff, U., Wijaya, A., Arif, R., Tarigan, R., & Sukmawinata, E. (2021). Comparison of colorimetric-based rabies postvaccination antibody titer detection using elisa reader and mobile phone camera. *Jurnal Veteriner*, *22*(1), 79–85. https://doi.org/10.19087/jveteriner.2021.22.1.79

Raghav, R., & Srivastava, S. (2016). Immobilization strategy for enhancing sensitivity of immunosensors: L-Asparagine-AuNPs as a promising alternative of EDC-NHS activated citrate-AuNPs for antibody immobilization. *Biosensors and Bioelectronics*, *78*, 396–403. https://doi.org/10.1016/j.bios.2015.11.066

Sohrabi, C., Alsafi, Z., O'Neill, N., Khan, M., Kerwan, A., Al-Jabir, A., Iosifidis, C., & Agha, R. (2020). World Health Organization declares global emergency: A review of the 2019 novel coronavirus (COVID-19). *International Journal of Surgery*, *76*(February), 71–76. https://doi.org/10.1016/j.ijsu.2020.02.034

Vashist, S. K. (2012). Comparison of 1-Ethyl-3-(3-Dimethylaminopropyl) Carbodiimide Based Strategies to Crosslink Antibodies on Amine-Functionalized Platforms for Immunodiagnostic Applications. *National Library of Medicine*, *2*(3) 23–33. https://doi.org/10.3390/diagnostics2030023

Wen, T., Huang, C., Shi, F. J., Zeng, X. Y., Lu, T., Ding, S. N., & Jiao, Y. J. (2020). Development of a lateral flow immunoassay strip for rapid detection of IgG antibody against SARS-CoV-2 virus. *Analyst*. *145*(15), 5345–5352. https://doi.org/10.1039/d0an00629g

Widyasari, D. A., Kristiani, A., Randy, A., Manurung, R. V., Dewi, R. T., Andreani, A. S., Yuliarto, B., & Jenie, S. N. A. (2022). Optimized antibody immobilization on natural silica-based nanostructures for the selective detection of E. coli. *RSC Advances*, *12*(33), 21582–21590. https://doi.org/10.1039/d2ra03143d

Xu, X., Chen, P., Wang, J., Feng, J., Zhou, H., Li, X., Zhong, W., & Hao, P. (2020). Evolution of the novel coronavirus from the ongoing Wuhan outbreak and modeling of its spike protein for risk of human transmission. *Science China Life Sciences*, *63*(3), 457–460. https://doi.org/10.1007/s11427-020-1637-5